Quantifying the risk posed by potential Earth impacts

Steven R. Chesley[1], Paul W. Chodas

Jet Propulsion Laboratory, California Institute of Technology

Andrea Milani

Dipartimento di Matematica, Università di Pisa, Pisa, Italy

Giovanni B. Valsecchi

IASF-CNR, Rome, Italy

and

Donald K. Yeomans

Jet Propulsion Laboratory, California Institute of Technology

Revised submission to Icarus for Asteroids 2001 special issue.

ABSTRACT

Predictions of future potential Earth impacts by Near-Earth Objects (NEOs) have become commonplace in recent years, and the rate of these detections is likely to accelerate as asteroid survey efforts continue to mature. In order to conveniently compare and categorize the numerous potential impact solutions being discovered we propose a new hazard scale that will describe the risk posed by a particular potential impact in both absolute and relative terms. To this end we measure each event in two ways, first without any consideration of the event's time proximity or its significance relative to the so-called background threat, and then in the context of the expected risk from other objects over the intervening years until the impact. This approach is designed principally to facilitate communication among astronomers, and it is not intended for public communication of impact risks. The scale characterizes impacts across all impact energies, probabilities and dates, and it is useful, in particular, when dealing with those cases which fall below the threshold of public interest. The scale also reflects the urgency of the situation in a natural way, and thus can guide specialists in assessing the computational and observational effort appropriate for a given situation. In this paper we describe the metrics introduced, and we give numerous examples of their application. This enables us to establish in rough terms the levels at which events become interesting to various parties.

Subject headings: ASTEROIDS, COMETS

[1]`steven.chesley@jpl.nasa.gov`

Proposed Running Head: Quantifying Earth Impact Risks

Correspondence Address:

Steven R. Chesley

JPL, M/S 301-150

4800 Oak Grove

Pasadena, CA 91109

(818) 354-9615, Fax: 393-6388

steven.chesley@jpl.nasa.gov

1. Introduction

Recent years have seen substantial advances in efforts to monitor the catalog of discovered asteroids and comets for those that might pose a threat to the Earth. These advances have taken place both in the theory of detecting and analyzing encounters, as well as in the level of professional and public interest in the problem. As a result there have been numerous detections of asteroid orbital solutions that lead to an Earth impact, generally several decades in the future and with very remote impact probabilities. Indeed, such detections are occurring at such a frequent rate that they are now becoming routine. This situation has created the need among impact specialists for a means of systematically measuring the importance, both relative and absolute, of so many cases in order to put them in their proper context. In particular, there is the need for a method of discerning the appropriate amount of computational and observational resources that should be dedicated to the problem when a potential collision solution consistent with the available observations is detected.

Any scheme designed to measure the importance of a potential impact should consider at least three general factors, each of which have roughly equal importance.

Impact Date. The time until the event determines the time available to react to the threat, which strongly influences the appropriate response. Clearly, high probability impacts taking place at some months, years, decades, centuries, or millennia in the future would each lead to very different threat mitigation strategies and levels of public interest.

Impact Energy. The consequences of the impact, should it occur, are clearly a key consideration in determining the proper professional and public response. Impacts have the potential of local, regional or global destruction. Other impacts, where the object is unlikely to cause any surface damage at all, may yet be of considerable scientific importance.

Impact Probability. The likelihood that the impact will actually occur is also of obvious importance. In particular, the significance of a predicted impact event relative to the mean impact frequency can indicate the level of interest appropriate to the situation.

The Torino Scale has been established as a "tool for *public* communication and assessment for asteroid and comet impact hazard predictions in the next century" (Binzel 2000, original emphasis; see also `http://impact.arc.nasa.gov/torino`). Avoiding complexity is appropriate, indeed necessary, when designing a scale targeted for public communication of risk, and the Torino Scale does present a clear and very simple measure of the hazard posed by a potential collision using a ten point integer scale. However, the simplicity of the Torino Scale makes it relatively unsuited for use by specialists in categorizing large numbers of events and in prioritizing objects for observation and analysis. There are several aspects of the Torino Scale that are problematic for these purposes:

1. The length of time until the predicted impact is not incorporated into the scale itself, and the impact date is required as an auxiliary item for proper interpretation, a point that is emphasized by Binzel (2000). This means that similar scenarios receive the same score whether the impact is in 90 days or 90 years. Furthermore, the scale is officially valid only for impacts that would occur within the next 100 years; impacts farther in the future have an indeterminate value on the Torino Scale.

2. Another difficulty is the use of an integer scale, which makes it impossible to recognize when events that have the same scale value are actually quite far apart. Conversely, two events that are practically indistinguishable may fall on opposite sides of a boundary, and thus appear to have markedly different importance. This problem is

compounded by the fact that the various regions associated with each integer value of the scale are arranged in a nonuniform manner, so that adjacent regions do not necessarily have consecutive integer values. While this approach may be appropriate for communicating with the public about infrequent events, an easily computed scale that is not only continuous, but smooth, and that stems from a simple algorithm or equation is preferable for handling large number of encounters in an automatic manner.

3. The Torino Scale assigns a zero value to all impacts with energy below 1 MT, no matter the probability. It also gives the value zero to all impact probabilities that fall well below the threshold of widespread public interest. This approach is appropriate if the public communication of the hazard to the Earth is the only objective, but it can be desirable to carefully consider potential impacts from very small objects, or from large objects at very low probabilities, to see, from a scientific perspective, how they compare to the expected impact flux from that size range and, from an operational perspective, to gauge the level of effort appropriate to the situation.

None of the foregoing points should be construed to imply that the Torino Scale is inadequate for its stated purpose. Indeed, while each of these may be viewed as a deficiency by specialists attempting to use it for more sophisticated purposes than it was designed, these same points make the Torino Scale more effective for communicating impact risks to a very wide and diverse audience. In any case, we believe a more robust and complex scale that addresses the issues listed above would aid communication among impact hazard experts, and would be of significant value to the professional NEO community.

In this paper we propose a system that smoothly characterizes impact hazards across the entire range of impact dates, energies and probabilities. We will describe two scales, one addressing the *intrinsic* risk, independent of time scale and background hazard, the other measuring the *relative* risk by comparing the intrinsic risk to the background threat. Each has a different interpretation, and together they provide useful insight into the nature and seriousness of a given threat.

The intrinsic risk is simply the probabilistic or expected energy flux from the potential collision in question. The scale used to relate the relative risk compares the intrinsic risk to the statistically expected energy flux from collisions at similar energy levels, integrated over the time interval until the potential collision. We show that this can be equivalent to comparing the impact probability to the integrated background impact probability for events at that energy level and higher.

This particular metric is certainly not new. The scheme has been proposed by several individuals, both publicly and privately, in discussions surrounding the adoption of the Torino Scale for public risk communication. Indeed, it was even offered by Binzel (2000) as one example of a possible metric that may be of value for specialists. We agree, and our purpose in presenting this scheme is to establish it both in the professional vernacular and in the published literature of our field.

The following development comprises two parts, definition and discussion. In the next section we describe the proposed hazard metrics and suggest some techniques for computing them uniformly. In Section 3 we consider many previous cases of potential impact and offer rough guidelines to characterize future results.

2. Development of the scale

The scheme we propose has two fundamental components. First we define a metric, which we call the *expected energy*, that measures the hazard posed by the event itself, without any reference to the background risk or to the time frame of the collision. Next we place the event in the context of the integrated background hazard over the intervening years until the potential impact. This second element, termed the *normalized risk*, is the most important component, but both convey distinct and relevant information.

2.1. Impact Energy

The energy released by a collision is, for all practical purposes, entirely kinetic, expressed in the usual form

$$E = \frac{1}{2} M V^2 .$$

The impact energy will be poorly defined in most cases due to substantial uncertainty in the object's mass M. On the other hand, the impact velocity V will be available to high precision since the impact trajectory is known for any given impact. Below we discuss separately each of these two terms in the energy equation.

While the most precise value for V is the one obtained from the output of the numerical integration of an impact solution, it is often more convenient, and entirely suitable, to obtain the impact velocity with the equation

$$V^2 = V_\infty^2 + V_e^2 \, ,$$

where V_∞ is the hyperbolic excess velocity of the object relative to the Earth and V_e is the Earth escape velocity, for which we have

$$V_e^2 = \frac{2GM_\oplus}{r_\oplus} \simeq (11.18 \text{ km/s})^2 \, .$$

Here we have used the mass constant $GM_\oplus$ and equatorial radius $r_\oplus$ of the Earth. For objects on heliocentric orbits V_∞ can be conveniently computed from Öpik's encounter theory (Öpik 1976) for a given set of orbital elements according to

$$V_\infty^2 = \frac{GM_\odot}{a_\oplus} \left[3 - \frac{a_\oplus}{a} - 2\sqrt{\frac{a(1-e^2)}{a_\oplus}} \cos i \right] ,$$

where $GM_{\odot}$ is the mass constant of the sun, $a_{\oplus} = 1\,\mathrm{AU}$ is the semimajor axis of the Earth, and a, e and i are, respectively, the semimajor axis, eccentricity, and inclination of the impactor's heliocentric orbit. Öpik's theory does require that the small body be hyperbolic relative to the geocentric frame, but for objects on weakly-bound elliptic geocentric orbits V_{∞} can be assumed zero. This approach also assumes the planet has a low eccentricity, which is entirely warranted for Earth impacts. Any errors induced in the Öpik approximation are negligible compared to the uncertainty in the mass determination of the object, to which we now turn.

The mass of an asteroid or comet is very difficult to obtain. The only accurate means is to carefully monitor the trajectory of a test particle as it is deflected during a close encounter with the target body, or as it orbits the target body. Several asteroid masses have been determined in this way, based on asteroid-asteroid encounters (e.g., Michalak 2000), perturbations on planets (Standish 2000), natural satellites of asteroids (Belton et al. 1996; Merline et al. 1999, 2000; Margot et al. 2001), and spacecraft flybys (Yeomans et al. 1997, 1999). The most precise asteroid mass determination to date was obtained during the year-long NEAR-Shoemaker orbital mission around 433 Eros (Yeomans et al. 2000).

In the absence of an accurate mass determination, the mass must be inferred from the size, shape, and density of an object, but for all potential impactors discovered to date, none of this information has been directly available, and this trend is likely to continue since the vast majority of potential impacts are associated with poorly observed objects. Typically, the only information available is the absolute magnitude H of the object, which relates its intrinsic brightness. In such circumstances we are forced to assume a homogeneous spherical object with density ρ, diameter D, and mass given by

$$M = \frac{\pi}{6}\,\rho D^3\,.$$

Given H and the albedo p_V, the diameter can be computed from the definition of albedo according to

$$D = 1329 \times 10^{-\frac{H}{5}}\, p_V^{-\frac{1}{2}}\,.$$

The principal source of error in the size of the object generally arises from the albedo uncertainty. However, the computed value of H can easily be wrong by a half magnitude or more since several simplifying assumptions are made about the object's phase relation (Bowell et al. 1989), and the computation typically assumes a flat light curve, which in unusual cases can have amplitudes of even a full magnitude. Furthermore, even if the photometric modeling is sufficient the available photometry is often of lower accuracy, which can also lead to errors on the order of a several tenths of a magnitude for poorly observed asteroids.

The near-Earth asteroid (NEA) population comprises numerous spectral classes. Table 1 lists the main classes along with very rough estimates of their respective contributions to the NEA population and characteristic values for their albedo and density. From the above equations it is clear that the mass varies linearly with ρ and $p_V^{-\frac{3}{2}}$, and the combined effect of these two highly uncertain parameters is registered through the product $\rho\, p_V^{-\frac{3}{2}}$. The respective values for $\rho\, p_V^{-\frac{3}{2}}$ are listed in the table, and it is remarkable that they differ only by a factor of a few. Crudely speaking, the darker C-class objects, which will be larger for a given H, compensate by having lower densities. This can only be regarded as an accident of nature, but, for our good luck, we are able to estimate NEA masses in most cases to within a factor of ~ 2 given only H.

With the absence of physical observations that is typical of objects with very short observed arcs, in particular for recently discovered objects, it is inescapable that there will be errors in the mass determination, yet there may still be a need to estimate the hazard posed by an object. To handle this situation, which is certainly the norm, we propose to establish standard values for the term $\rho\, p_V^{-\frac{3}{2}}$ to be used in computing the impact risk for both asteroids and comets. The values we have selected are listed in Table 1, where the NEA standard value is obtained from a weighted mean using the population fraction based on absolute magnitude, which best represents the known population. We use the word "standard" somewhat loosely; the bimodal asteroid population will likely have a very small fraction of objects for which our standard values are actually appropriate. However, the standard values will give reasonably good results in an average sense for all classes as indicated by the tabulated values of $\rho\, p_V^{-\frac{3}{2}}$. Of course, if more accurate information on the physical characteristics of the body becomes available it should be used in the object's mass estimation. It is important, however, in such cases that the actual values used be explicitly specified when describing the impact hazard based on the methods described in this paper, because the standard values in Table 1 are assumed otherwise. This standardization should facilitate comparisons among various research groups, as well as among different objects.

2.2. Impact Probability

The probability of an impact actually occurring is an externally derived input for the impact hazard evaluation. At the first level, every dynamically distinct route to impact should undergo a separate hazard analysis based upon the probability for that particular event. (The results from multiple analyses can later be summed if desired, as discussed below.) Present methods for detecting potential collisions and evaluating the probability of impact are described in several publications (e.g., Chodas and Yeomans 1999a,b; Milani et al. 2000, 2002). The methods all share the deficiency that the probabilities computed are uncertain, possibly by an order of magnitude or more, but generally much less. This is largely due to the uncertainty of the error statistics of the object's astrometric observations, which translates, often nonlinearly, into the uncertainty of the orbit determination, and finally into uncertainty of the range possible of orbits compatible with the observations.

Recent research aimed at improving the modeling of observational errors in the orbit determination process is ongoing (Carpino et al. 2001), and should eventually permit more accurate impact probability computations. Moreover, beyond this fundamental difficulty, there are several approximations with the probability computation itself that can come into play, and these can further corrupt the probability estimate by a factor of a few.

2.3. Intrinsic Hazard

Given the impact energy E and impact probability P_I, we can compute the *expected energy* $\tilde{E}$ for a particular event, which we define to be the product of the two. That is,

$$\tilde{E} = P_I \, E \, ,$$

which is in a real sense a probabilistic energy; it is the average energy that would be expected to be delivered given a large statistically consistent sampling of the entire range of potential orbits. This value is limited to the encounter in question, which is uniquely defined by the dynamical route to impact and the time of impact. If other distinct impact events are possible, they must be handled separately, but the expected energy from numerous collision opportunities can be summed to form a cumulative expected energy. This value realistically indicates the aggregate threat posed by the object with no context in time or background hazard.

The expected energy is an appropriate way to evaluate an individual event in terms of its human, economic, and environmental threat. On the other hand the Torino Scale, which operates in the same parameter space, is based (more or less) on lines of constant $E \, P_I^{-3/2}$ (see Figure 1). This approach puts the event in the context of what is "normal," but it does not accurately reflect the intrinsic hazard. Because of this, the Torino Scale tends to deemphasize the threat posed by very large impacts, while it raises smaller impacts to a level of concern that is perhaps more than necessary based on the potential threat alone. This can be viewed as a sort of short cut, necessitated by the drive for simplicity, in the sense that the Torino Scale strives to simultaneously reflect both the intrinsic and relative hazards.

The expected energy can also be useful in guiding the search for potential impacts. Instead of monitoring for all objects down to a fixed level of impact probability as is done now, it may be preferable to search down to a prescribed level of $\tilde{E}$. This implies that larger objects would require a more thorough and computationally expensive search for impactors. Such an approach is reasonable, and could offer a more optimal monitoring strategy from the perspective of Earth protection.

2.4. Background Hazard

It is important to measure the threat posed by a particular impact or object relative to the statistical threat, that is the threat from the entire asteroid and comet population averaged over very long time spans. To proceed we need to adopt some relation to model this *background hazard*, and for this purpose we rely on the work of Chapman and Morrison (1994). The frequency f_B of Earth impacts with energies greater than E reported by Chapman and Morrison is given by the circles in Fig. 2. We have selected the simple exponential function

$$f_B = \frac{3}{100}\, E^{-4/5}\, \mathrm{yr}^{-1},$$

where E is measured in MT (megatons of TNT, $1\,\mathrm{MT} = 4.2 \times 10^{15}\mathrm{J}$), as an adequate representation of the terrestrial impact frequency (solid line in Fig. 2). For comparison we also include the impact frequency used by Binzel (2000) in formulating the Torino Scale (dashed line). In their report, Chapman and Morrison ultimately used the result of Shoemaker (1983), which is largely based on the lunar cratering record, and we note that this criteria is distinct from the threat associated with the *undiscovered* component of the asteroid population. The hazard due to only the undiscovered objects, which is also sometimes referred to as the "background" hazard, decreases with time as the completeness of the catalog of discovered asteroids improves, and is therefore not suitable as a reference for impact hazards.

It is reasonable to measure the background hazard by either counting all of the impacts at greater energies according to the above expression, or by estimating the energy flux for impacts at comparable energies. In the following development we shall consider both interpretations, and ultimately unify them, but first we need an expression for the energy flux, given the impact flux above. We assume that for low enough values, the impact frequency (per year) is equivalent to the annual probability of impact for events at that energy level or greater. This interpretation allows us to deduce the annual impact probability density $\gamma(E)$ at a given energy E

$$\gamma(E) = \frac{3}{125} E^{-9/5}\,\mathrm{MT}^{-1},$$

so that $\int_E^\infty \gamma(E)\,dE$ gives the expression for f_B above. With the impact probability density we can now compute the expected annual energy flux $\tilde{E}_B$ for a given energy band of width $(\alpha - \alpha^{-1})\,E$ according to

$$\begin{aligned} \tilde{E}_B(E,\alpha) &= \int_{E/\alpha}^{\alpha E} E\gamma(E)\,dE \\ &= \frac{3}{25}(\alpha^{1/5} - \alpha^{-1/5})E^{1/5}\,\mathrm{MT}. \end{aligned}$$

2.5. Relative Hazard

Now, with a definition of the background hazard in hand we can consider the ratio of the event's expected energy to the background energy flux from events at similar energies in the intervening years before the potential impact

$$R_\alpha = \frac{\tilde{E}}{\tilde{E}_B(E,\alpha)\,\Delta T}.$$

Here ΔT is the number of years remaining until the event. Using the previous definitions, the above reduces to

$$R_\alpha = \frac{P_I}{\kappa\, f_B\, \Delta T}\,,$$

where

$$\kappa = 4\,(\alpha^{1/5} - \alpha^{-1/5}).$$

Thus as the energy band used for comparison widens, κ increases, and the relative hazard diminishes. If we set $\kappa = 1$ then we find

$$\alpha = \left(\frac{1+\sqrt{65}}{8}\right)^5 \simeq 1.865\,,$$

which implies an energy band of width $(\alpha - \alpha^{-1})\,E \simeq 1.329\,E$. Adopting this value of α for the present scale, we define the *normalized risk* as

$$R = \frac{P_I}{f_B\,\Delta T}\,.$$

The above expression is precisely the metric M already suggested for professional use by Binzel (2000), and the foregoing development has had the ultimate objective of providing a justification and interpretation for its use. Specifically, the normalized risk has two possible interpretations. It is the expected energy for the event in question weighed against the expected energy flux from similar-sized events in the intervening years until the impact. On the other hand, it is also the impact probability weighed against the probability of a larger impact in the intervening years until the impact. In either interpretation, the background risk is accumulated from the present time until the date of the potential impact.

In the potential impacts discovered to date, the normalized risk R is often a very small number, ranging from below 10^{-11} to upwards of 10^{-1}. For this reason we use the logarithm to define the present hazard scale

$$\mathcal{P} = \log_{10} R\,.$$

The cumulative concept described above for expected energy can also be applied to the to the normalized risk. The values of R from numerous potential impacts from a single object can be accumulated to measure the aggregate normalized risk posed by that object. Moreover, the aggregate risk from several objects can even be accumulated in the same way to give a meaningful measure of the hazard posed by all known threats. In a theoretical and statistical sense the aggregate normalized risk from the entire asteroid and comet population should be precisely unity. In practice this value will generally be much less because collision monitoring can only search relatively short time periods 50–100 years in the future; however, it could rise to a level even much greater than one if a near-term event with high expected energy is discovered.

3. Examples and Discussion

To provide some feeling for the point at which the metrics introduced above should become in some sense "interesting" we consider here some of the numerous previous and current potential impact detections. To this end, we have selected the 23 objects in Table 2 by including most of the potential impactors listed at the time of this writing on the NEODyS Risk Page [2], plus all objects that have generated some level of discussion among the interested public, and a few other interesting objects. Table 2 itemizes the selected objects, along with associated parameters of interest that do not depend upon the date

[2] See `http://newton.dm.unipi.it/neodys`. We have excluded objects that are presently under continuing active observation. See also `http://neo.jpl.nasa.gov/risk` for an independent listing of future impact possibilities.

or probability of impact. In Table 3 we tabulate the respective data for each potential impact, as well as cumulative values for each object, when applicable. This selection of objects and impact opportunities is by no means complete. In fact, the data are extracted from several disparate sources, using different software, observation weighting, and analysis techniques. This is therefore neither an exhaustive nor self-consistent listing of potential impact detections to date, and we use it only to establish the present scale in the context of past experience.

The main point to be drawn from Table 2 is the large range of diameters and impact energies. Three objects have impact energies at the level nominally required for a global catastrophe (Chapman and Morrison 1994), while at least four objects are so small that they would be unlikely to cause any surface damage whatsoever. Although our approach does not place a lower bound on the kinetic energy for which objects may be of interest, proper interpretation of a very probable collision requires consideration of the energy that would be released by the impact if it were to occur. It is worth noting that the very low V_∞ of 2000 SG_{344} and 2001 GP_2 make them rather unusual among the NEA population, and the possibility that they are man-made has not been ruled out (Chodas and Chesley 2001). If either is eventually determined to be artificial the impact hazard associated with the object would vanish.

The interpretation of Table 3 is more interesting. First we point out that there are eight objects with "nuclear" sized values for expected energy ($\tilde{E} > 10\,\mathrm{kT}$), for which serious damage may be statistically expected. (And another three objects have expected energies in the range 1–10 kT.) For collisions in the next several decades, such values should probably at least raise eyebrows within the professional impact hazard community, and should also warrant aggressive observational efforts to improve the orbit of the object in question. Except for 1994 WR_{12}, which is badly lost, all eight objects with potential impacts at large values of $\tilde{E}$ detected to date have eventually been eliminated due to new observations obtained from archival images (1997 XF_{11} and 1999 AN_{10}), previously unlinked observations (1998 KM_3), or targeted followup efforts (2000 PN_9, 2001 PM_9, 2001 VK_5, 2001 WN_5 and, to some extent, 1999 AN_{10}).

Thirteen objects not being currently observed have potential impacts (i.e., using all of the presently available data) as of Jan. 1, 2002. Of these, nine are lost, including 1994 WR_{12}, which is the only object posing a meaningful hazard for which potential impacts cannot be ruled out at present. The four other objects include 2000 SG_{344} and 2001 GP_2, which may not even be natural bodies (and therefore their orbits may be significantly affected by non gravitational perturbations) as well as 2001 BA_{16} and 2001 AV_{43}, which could be recovered at the predicted close approaches in the years 2012 and 2013, respectively. On top of these objects, which are more or less permanently listed on the Risk Pages, there are temporary ones, first listed there while they are still observable. In most cases the objects disappear from the Risk Pages when, after a few days of additional observations, all detected possibilities of impact can be ruled out.

The significance of a potential impact event will generally be well characterized solely by $\mathcal{P}$. We have not yet discovered a case for which $\mathcal{P} > 0$, i.e., a situation more threatening than the background hazard, but if this did occur it should certainly rise to the level of public awareness, even concern, depending on the time frame and expected energy involved. (Such cases will generally also have nonzero values on the Torino Scale so long as the collsion is some years away.) However, there are five objects with events for which $\mathcal{P} > -2$ and some of these have been of distinct professional and public interest. We believe that such cases should continue to be of moderate interest to the public at large. Additionally, there are six objects (including the lost 1994 WR_{12}) with events in the range $-3 < \mathcal{P} < -2$. Several of these have also generated some public discussion, and it is reasonable that the more interested public be made aware of such cases. There are numerous events that fall in the range of $-5 < \mathcal{P} < -3$, and we judge these cases to be of interest to professionals charged with monitoring for impact risks, and, in particular, to those responsible for orchestrating appropriate observational campaigns. However, since the frequency of detections in this range will continue to be at the level of several per year, speaking in very rough terms, we do not see them as warranting public concern. Events at even lower levels will likely be of academic interest only, e.g., for testing impact prediction algorithms.

For potential impact events occuring a few decades in the future a rough guideline is that if $\mathcal{P} > -2$ then the Torino Scale value will be nonzero. Of the eleven events in Table 3 for which $\mathcal{P} > -2$ only three fail to satisfy this simple rule, this because they would occur relatively close in time, thus raising the value of $\mathcal{P}$. Conversely, of the eleven Torino Scale 1 events in the Table there are three with $\mathcal{P} < -2$, generally because the event is several decades into the future, or in the case of 2000 SG_{344}, because the object has a small impact energy. This stems largely from the fact that, as was mentioned earlier, the Torino Scale tends to give greater emphasis to events with lower energy values, when compared with the expected energy.

We consider separately the asteroid 433 Eros as an extreme test of the methods outlined in this paper. Michel et al. (1996) report that roughly 3/8 of Eros clones evolve to Earth-crossing orbits, typically in around a million years. Since the probability of impact at any given node crossing is around 10^{-5} we can "predict" an Earth-Eros collision with probability of impact $\sim 10^{-6}$ around a million years from now. In this case we find $\tilde{E} = 160\,\mathrm{MT}$, but $\mathcal{P} = -3.9$, indicating that the event may be of very serious concern for future Earthlings, but not for us, and in fact is quite unremarkable relative to the background hazard. Alternatively, the same authors report (Michel et al. 1998) that Eros has $\sim 5\%$ chance of impact over the next few billion years, which leads to $\tilde{E} \simeq 10^7\,\mathrm{MT}$ (!)

and $\mathcal{P} \simeq -2.2$, but the final conclusion remains the same.

4. Nomenclature

In order for the scale described in this paper to be immediately useful within the professional NEO community we believe it should have a distinctive name. Inspired by the naming of the Torino Impact Hazard Scale, we propose the name “Palermo Technical Impact Hazard Scale” for the metric $\mathcal{P}$, in recognition of the historic contribution of the Palermo observatory to asteroid science, namely the first discovery of an asteroid, as well as in recognition of the location of the “Asteroids 2001” international conference where we have first presented these results.

Acknowledgements

We are grateful to Alan Harris (JPL) for numerous helpful discussions, and in particular for his assistance with the preparation of Table 1. This research was conducted at the Jet Propulsion Laboratory, California Institute of Technology, under a contract with the National Aeronautics and Space Administration. A.M. and G.B.V. acknowledge partial support from the Italian Space Agency.

REFERENCES

Belton, M. J. S., Mueller, B. E. A., D'Amario, L. A., Byrnes, D. V., Klaasen, K. P., Synnott, S., Breneman, H., Johnson, T. V., Thomas, P. C., Veverka, J., Harch, A. P., Davies, M. E., Merline, W. J., Chapman, C. R., Davis, D., Denk, T., Neukum, G., Petit, J., Greenberg, R., Storrs, A., and Zellner, B. (1996). The discovery and orbit of 1993 (243)1 Dactyl. *Icarus*, 120:185–199.

Binzel, R. P. (2000). The Torino Impact Hazard Scale. *Planet. Space Sci.*, 48:297–303.

Bowell, E., Hapke, B., Domingue, D., Lumme, K., Peltoniemi, J., and Harris, A. W. (1989). Application of photometric models to asteroids. In *Asteroids II*, pages 524–556. Univ. Arizona Press, Tucson.

Carpino, M., Milani, A., and Chesley, S. R. (2001). Error statistics of asteroid optical astrometric observations. *Icarus*. submitted.

Chapman, C. R. and Morrison, D. (1994). Impacts on the earth by asteroids and comets: assessing the hazard. *Nature*, 367:33–40.

Chodas, P. W. and Chesley, S. R. (2001). 2000 SG344: The story of a potential earth impactor. In *AAS/Division of Dynamical Astronomy Meeting*.

Chodas, P. W. and Yeomans, D. K. (1999a). Orbit determination and estimation of impact probability for near-Earth objects. Paper AAS 99-002, 21st Annual AAS Guidance and Control Conference, Breckenridge, Colorado.

Chodas, P. W. and Yeomans, D. K. (1999b). Predicting close approaches and estimating impact probabilities for near-Earth objects. Paper AAS 99-462, AAS/AIAA Astrodynamics Specialists Conference, Girdwood, Alaska.

Harris, A. W. (1989). The H-G asteroid magnitude system: Mean slope parameters. In *Lunar and Planetary Science Conference*, volume 20, pages 375–376.

Margot, J. L., Nolan, M. C., Benner, L. A. M., Ostro, S. J., Jurgens, R. F., Giorgini, J. D., Slade, M. A., and Campbell, D. B. (2001). Radar observations of binary asteroid 2000 DP_{107}. In *Lunar and Planetary Science Conference*, volume 32, pages 1754+.

McFadden, L.-A., Tholen, D. J., and Veeder, G. J. (1989). Physical properties of Aten, Apollo and Amor asteroids. In Binzel, R. P., Gehrels, T., and Matthews, M. S., editors, *Asteroids II*, pages 442–467. Univ. Arizona Press, Tucson.

Merline, W. J., Close, L. M., Dumas, C., Chapman, C. R., Roddier, F., Menard, F., Slater, D. C., Duvert, G., Shelton, C., and Morgan, T. (1999). Discovery of a moon orbiting the asteroid 45 Eugenia. *Nature*, 401:565+.

Merline, W. J., Close, L. M., Dumas, C., Shelton, J. C., Menard, F., Chapman, C. R., and Slater, D. C. (2000). Discovery of companions to asteroids 762 Pulcova and 90 Antiope by direct imaging. In *AAS/Division of Planetary Sciences Meeting*, volume 32, pages 1306+.

Michalak, G. (2000). Determination of asteroid masses — I. (1) Ceres, (2) Pallas and (4) Vesta. *A&A*, 360:363–374.

Michel, P., Farinella, P., and Froeschlé, C. (1998). Dynamics of Eros. *AJ*, 116:2023–2031.

Michel, P., Froeschlé, C., and Farinella, P. (1996). Dynamical evolution of two near-Earth asteroids to be explored by spacecraft: (433) Eros and (4660) Nereus. *A&A*, 313:993–1007.

Milani, A., Chesley, S. R., Chodas, P. W., and Valsecchi, G. B. (2002). *Asteroids III*, chapter Asteroid Close Approaches: Analysis and Potential Impact Detection. University of Arizona Press. in press.

Milani, A., Chesley, S. R., and Valsecchi, G. B. (2000). Asteroid close encounters with earth: risk assessment. *Planet. Space Sci.*, 48:945–954.

Öpik, E. J. (1976). *Interplanetary encounters : close-range gravitational interactions.* Elsevier Scientific Pub. Co., New York.

Rahe, J., Vanysek, V., and Weissman, P. (1994). Properties of cometary nuclei. In Gehrels, T., editor, *Hazards Due to Comets & Asteroids*, pages 597–643. Univ. Arizona Press, Tucson.

Shoemaker, E. M. (1983). Asteroid and comet bombardment of the earth. *Annual Review of Earth and Planetary Sciences*, 11:461–494.

Standish, E. M. (2000). Recommendation of DE405 for 2001 Mars Surveyor and for Cassini. Technical Report IOM 312.F-00-107b, Jet Propulsion Laboratory.

Yeomans, D. K., Antreasian, P. G., Barriot, J.-P., Chesley, S. R., Dunham, D. W., Farquhar, R. W., Giorgini, J. D., Helfrich, C. E., Konopliv, A. S., McAdams, J. V., Miller, J. K., Owen, W., Scheeres, D. J., Thomas, P. C., Veverka, J., and Williams, B. G. (2000). Radio science results during the NEAR-Shoemaker spacecraft rendezvous with Eros. *Science*, 289:2085–2088.

Yeomans, D. K., Antreasian, P. G., Cheng, A., Dunham, D. W., Farquhar, R. W., Gaskell, R. W., Giorgini, J. D., Helfrich, C. E., Konopliv, A. S., McAdams, J. V., Miller, J. K., Owen, W., Thomas, P. C., Veverka, J., and Williams, B. G. (1999). Estimating the mass of asteroid 433 eros during the NEAR spacecraft flyby. *Science*, 285:560–561.

Yeomans, D. K., Barriot, J.-P., Dunham, D. W., Farquhar, R. W., Giorgini, J. D., Helfrich, C. E., Konopliv, A. S., McAdams, J. V., Miller, J. K., Owen, W., Scheeres, D. J., Synnott, S. P., and Williams, B. G. (1997). Estimating the mass of asteroid 253 Mathilde from tracking data during the NEAR flyby. *Science*, 278:2106–2109.

This manuscript was prepared with the AAS LaTeX macros v5.0.

Table 1. Near-Earth Object Categories and Properties.

Category	NEA fraction[a] % (> D)	NEA fraction[a] % (< H)	ρ (g/cm^3)	p_V	$\rho\, p_V^{-\frac{3}{2}}$ (g/cm^3)
C-class	45	16	1.3[b]	0.06[c]	88
S-class	45	62	2.7[b]	0.18[c]	35
M-class	5	4	5.3[b]	0.12[c]	127
E-class	5	18	2.7	0.40[c]	11
Standard NEA	···	···	(2.6)	(0.154)	43
Standard Comet	···	···	1.1[d]	0.04[d]	138

[a]The population fraction larger than a fixed diameter D is difficult to discern due to observational bias, but we believe these values are representative of the true population. The population fraction brighter than a given absolute magnitude H has been computed directly from the size-based fractions and albedos in the Table, and with the assumption that the population follows $N(> D) \propto D^{-2.4}$, which is consistent with our expression for f_B. This brightness-based fraction should represent in rough terms the observed population, and indeed the tabulated values agree remarkably well with the results of McFadden et al. (1989).

[b]Standish (2000)

[c]Harris (1989)

[d]Rahe et al. (1994)

Note. — In this table we have followed Harris (1989) by grouping similar spectral classes. Therefore, the C-class includes C, G, B, F, P, T and D, the S-class also includes Q and A, and the E-class includes E, V and R.

Table 2. Relevant Parameters for Objects of Interest.

Object	H	V_∞ (km/sec)	V (km/sec)	D (km)	M (kg)	E (MT)	f_B (yr^{-1})
2000 PN_9	15.93	31.05	33.00	2.20	1.5e+13	1.9e+06	2.9e-07
2001 BK_{41}	16.10	10.89	15.61	2.04	1.2e+13	3.4e+05	1.1e-06
1997 XF_{11}	16.51	13.64	17.64	1.69	6.6e+12	2.4e+05	1.5e-06
1999 AN_{10}	17.89	26.35	28.62	0.89	9.8e+11	9.5e+04	3.1e-06
2001 VK_5	17.76	18.59	21.70	0.95	1.2e+12	6.6e+04	4.2e-06
2001 WN_5	18.36	9.56	14.71	0.72	5.1e+11	1.3e+04	1.5e-05
2001 PM_9	18.45	9.01	14.36	0.69	4.5e+11	1.1e+04	1.8e-05
1999 RM_{45}	19.29	20.16	23.06	0.47	1.4e+11	9.0e+03	2.1e-05
1998 KM_3	19.40	17.91	21.11	0.45	1.2e+11	6.4e+03	2.7e-05
2000 BF_{19}	19.29	10.68	15.46	0.47	1.4e+11	4.0e+03	3.9e-05
1998 OX_4	21.33	12.55	16.81	0.18	8.4e+09	2.8e+02	3.3e-04
1994 UG	21.13	6.75	13.06	0.20	1.1e+10	2.2e+02	4.0e-04
2001 SB_{170}	22.41	22.33	24.97	0.11	1.9e+09	1.4e+02	5.8e-04
1994 WR_{12}	22.11	9.09	14.41	0.13	2.9e+09	7.1e+01	1.0e-03
1994 GK	24.20	15.69	19.26	0.05	1.6e+08	7.1e+00	6.3e-03
1995 CS	25.47	25.35	27.71	0.03	2.8e+07	2.5e+00	1.4e-02
2001 AV_{43}	24.30	4.41	12.02	0.05	1.4e+08	2.4e+00	1.5e-02
1997 TC_{25}	24.66	9.01	14.36	0.04	8.4e+07	2.1e+00	1.7e-02
2000 SG_{344}	24.79	1.90	11.34	0.04	7.1e+07	1.1e+00	2.8e-02

Table 2—Continued

Object	H	V_∞ (km/sec)	V (km/sec)	D (km)	M (kg)	E (MT)	f_B (yr^{-1})
2001 BA_{16}	25.83	4.73	12.14	0.02	1.7e+07	3.0e-01	7.9e-02
2001 GP_2	26.88	2.16	11.39	0.01	3.9e+06	6.1e-02	2.8e-01
1994 GV	27.47	8.42	14.00	0.01	1.8e+06	4.1e-02	3.9e-01
1991 BA	28.66	17.99	21.18	0.01	3.3e+05	1.8e-02	7.5e-01

Note. — Objects are sorted according to descending impact energy.

Table 3. Potential Impacts for Objects of Interest.

Year	P_I	$\tilde{E}$ (MT)	R	$\mathcal{P}$
2000 PN_9 (from 57 obs. 2000 Aug. 8–11)				
2046	1.5e-08	2.7e-02	1.2e-03	-2.94
2001 BK_{41} (from 21 obs. 2001 Jan. 19–26)				
2005	2.0e-08	6.8e-03	5.9e-03	-2.23
2019	8.0e-10	2.7e-04	4.1e-05	-4.38
2022	1.0e-10	3.4e-05	4.4e-06	-5.36
Cum.	2.1e-08	7.1e-03	5.9e-03	-2.23
1997 XF_{11} (from 98 obs. 1997 Dec. 6–1998 Mar. 4)				
2039	7.0e-07	1.7e-01	1.3e-02	-1.89†
2040	2.0e-05	4.9e+00	3.6e-01	-0.45†
2041	2.0e-06	4.9e-01	3.5e-02	-1.46†
2041	1.0e-07	2.4e-02	1.7e-03	-2.76
2043	2.0e-06	4.9e-01	3.3e-02	-1.48†
2047	4.0e-07	9.8e-02	6.1e-03	-2.22
2047	7.0e-08	1.7e-02	1.1e-03	-2.97
2048	6.0e-07	1.5e-01	8.9e-03	-2.05†
Cum.	2.6e-05	6.3e+00	4.6e-01	-0.34
1999 AN_{10} (from 114 obs. 1999 Jan. 13–May 27)				
2044	6.2e-06	5.9e-01	4.7e-02	-1.33†
2046	4.5e-07	4.3e-02	3.3e-03	-2.48

Table 3—Continued

Year	P_I	$\tilde{E}$ (MT)	R	$\mathcal{P}$
2047	2.0e-10	1.9e-05	1.4e-06	-5.85
Cum.	6.7e-06	6.3e-01	5.0e-02	-1.30
1999 AN_{10} (from 106 obs. 1999 Jan. 13–Feb. 20)				
2039	1.0e-09	9.5e-05	8.7e-06	-5.06
2001 VK_5 (from 47 obs. 2001 Nov. 11–18)				
2011	9.1e-06	5.9e-01	2.4e-01	-0.62†
2014	1.5e-06	9.7e-02	2.9e-02	-1.53†
2024	1.1e-07	6.9e-03	1.1e-03	-2.94
2024	1.3e-06	8.4e-02	1.4e-02	-1.86
2030	4.3e-07	2.8e-02	3.7e-03	-2.44
2033	7.9e-07	5.2e-02	6.1e-03	-2.21
2039	2.7e-07	1.8e-02	1.7e-03	-2.76
2045	9.1e-07	6.0e-02	5.1e-03	-2.30
Cum.	1.5e-05	9.5e-01	3.0e-01	-0.52
2001 WN_5 (from 41 obs. 2001 Nov. 20–Dec. 12)				
2031	6.5e-08	8.6e-04	1.5e-04	-3.83
2058	3.1e-06	4.1e-02	3.7e-03	-2.44
2065	1.4e-06	1.9e-02	1.5e-03	-2.83
2067	8.6e-09	1.1e-04	8.7e-06	-5.06
2070	6.7e-05	8.9e-01	6.5e-02	-1.19†

Table 3—Continued

Year	P_I	$\tilde{E}$ (MT)	R	$\mathcal{P}$
2075	2.8e-08	3.7e-04	2.5e-05	-4.60
2079	2.3e-08	3.0e-04	2.0e-05	-4.70
Cum.	7.2e-05	9.5e-01	7.0e-02	-1.15
2001 PM_9 (from 31 obs. 2001 Aug. 11–16)				
2005	1.7e-06	1.9e-02	3.2e-02	-1.49
2007	1.3e-06	1.4e-02	1.5e-02	-1.83
2009	5.8e-08	6.4e-04	4.8e-04	-3.32
2060	3.6e-08	3.9e-04	3.5e-05	-4.46
2062	6.8e-08	7.5e-04	6.5e-05	-4.19
Cum.	3.2e-06	3.5e-02	4.8e-02	-1.32
1999 RM_{45} (from 38 obs. 1999 Sep. 13–20)				
2042	3.0e-09	2.7e-05	3.6e-06	-5.44
2050	4.0e-09	3.6e-05	4.0e-06	-5.39
Cum.	7.0e-09	6.3e-05	7.6e-06	-5.12
1998 KM_3 (from 26 obs. 1998 May 24–Jun. 17)				
2069	1.1e-08	7.0e-05	6.0e-06	-5.22
2071	1.5e-07	9.8e-04	8.2e-05	-4.08
2071	3.5e-06	2.3e-02	1.9e-03	-2.72
2076	1.1e-06	6.9e-03	5.4e-04	-3.27
2077	3.6e-07	2.3e-03	1.8e-04	-3.75

Table 3—Continued

Year	P_I	$\tilde{E}$ (MT)	R	$\mathcal{P}$
Cum.	5.1e-06	3.3e-02	2.7e-03	-2.57
2000 BF_{19} (from 22 obs. 2000 Jan. 28–Feb. 4)				
2022	1.0e-06	4.0e-03	1.3e-03	-2.89
1998 OX_4 (from 21 obs. 1998 Jul. 26–Aug. 4)‡				
2038	2.6e-07	7.2e-05	2.2e-05	-4.66
2044	3.6e-07	1.0e-04	2.6e-05	-4.58
2046	5.0e-07	1.4e-04	3.5e-05	-4.46
2054	3.3e-09	9.3e-07	1.9e-07	-6.71
2078	1.4e-08	4.0e-06	5.7e-07	-6.24
2086	7.6e-09	2.2e-06	2.8e-07	-6.56
2095	4.2e-07	1.2e-04	1.4e-05	-4.86
2097	9.3e-08	2.6e-05	3.0e-06	-5.53
Cum.	1.7e-06	4.7e-04	1.0e-04	-4.00
1994 UG (from 15 obs. 1994 Oct. 28–Nov. 1)‡				
2044	6.0e-10	1.3e-07	3.6e-08	-7.44
2001 SB_{170} (from 29 obs. 2001 Sep. 18–Oct. 13)‡				
2073	3.1e-08	4.4e-06	7.7e-07	-6.11
1994 WR_{12} (from 24 obs. 1994 Nov. 26–Dec. 31)‡				
2071	2.5e-05	1.7e-03	3.6e-04	-3.44
2073	1.3e-05	9.4e-04	1.9e-04	-3.72

Table 3—Continued

Year	P_I	$\tilde{E}$ (MT)	R	$\mathcal{P}$
2074	1.6e-04	1.1e-02	2.2e-03	-2.66[†]
2075	1.8e-05	1.2e-03	2.4e-04	-3.61
2076	4.9e-05	3.5e-03	6.6e-04	-3.18
Cum.	2.7e-04	1.8e-02	3.7e-03	-2.44
1994 GK (from 18 obs. 1994 Apr. 7–10)[‡]				
2033	1.3e-08	9.2e-08	6.7e-08	-7.17
2061	7.3e-08	5.1e-07	2.0e-07	-6.71
2067	3.9e-07	2.8e-06	9.6e-07	-6.02
2070	1.8e-06	1.3e-05	4.2e-06	-5.37
2073	1.3e-06	9.2e-06	2.9e-06	-5.53
Cum.	3.6e-06	2.6e-05	8.3e-06	-5.08
1995 CS (from 14 obs. 1995 Feb. 4–7)[‡]				
2042	5.2e-06	1.3e-05	9.2e-06	-5.04
2001 AV_{43} (from 38 obs. 2001 Jan. 5–Feb. 1)[‡]				
2057	7.7e-08	1.8e-07	9.4e-08	-7.03
2057	1.1e-05	2.5e-05	1.3e-05	-4.89
2068	2.7e-09	6.4e-09	2.7e-09	-8.56
2078	1.4e-09	3.3e-09	1.2e-09	-8.91
Cum.	1.1e-05	2.5e-05	1.3e-05	-4.88
1997 TC_{25} (from 13 obs. 1997 Oct. 10–23)[‡]				

Table 3—Continued

Year	P_I	$\tilde{E}$ (MT)	R	$\mathcal{P}$
2078	3.0e-09	6.2e-09	2.3e-09	-8.63
2000 SG_{344} (from 23 obs. 1999 May 15–2000 Oct. 3)				
2030	2.0e-03	2.2e-03	2.5e-03	-2.59†
2000 SG_{344} (from 31 obs. 1999 May 15–2000 Oct. 3)‡				
2071	1.0e-03	1.1e-03	5.2e-04	-3.29
2001 BA_{16} (from 21 obs. 2001 Jan. 19–Feb. 28)‡				
2041	1.6e-04	4.8e-05	5.3e-05	-4.28
2051	5.5e-05	1.6e-05	1.4e-05	-4.85
2059	2.4e-06	7.2e-07	5.4e-07	-6.27
Cum.	2.2e-04	6.5e-05	6.8e-05	-4.17
2001 GP_2 (from 25 obs. 2001 Apr. 13–May 9)‡				
2062	6.0e-05	3.6e-06	3.5e-06	-5.45
2068	1.5e-05	8.8e-07	7.8e-07	-6.11
2072	8.5e-06	5.2e-07	4.3e-07	-6.37
Cum.	8.4e-05	5.0e-06	4.7e-06	-5.33
1994 GV (from 19 obs. 1994 Apr. 13–15)‡				
2036	2.2e-07	8.8e-09	1.6e-08	-7.78
2039	1.5e-04	6.0e-06	1.0e-05	-4.99
2044	9.5e-07	3.9e-08	5.8e-08	-7.23
2050	2.0e-07	8.1e-09	1.1e-08	-7.97

Table 3—Continued

Year	P_I	$\tilde{E}$ (MT)	R	$\mathcal{P}$
Cum.	1.5e-04	6.1e-06	1.0e-05	-5.00
1991 BA (from 7 obs. 1991 Jan. 18)‡				
2003	3.0e-06	5.4e-08	4.1e-06	-5.39
2010	1.5e-06	2.7e-08	2.5e-07	-6.60
2046	2.0e-10	3.6e-12	6.1e-12	-11.22
Cum.	4.5e-06	8.1e-08	4.4e-06	-5.36

Note. — For several objects in this table the list of potential impacts is rather extensive and the tabulated events are limited to the most significant cases.

†Torino Scale 1 events.

‡Reflects all available observations as of Jan. 1, 2002.

List of Figures

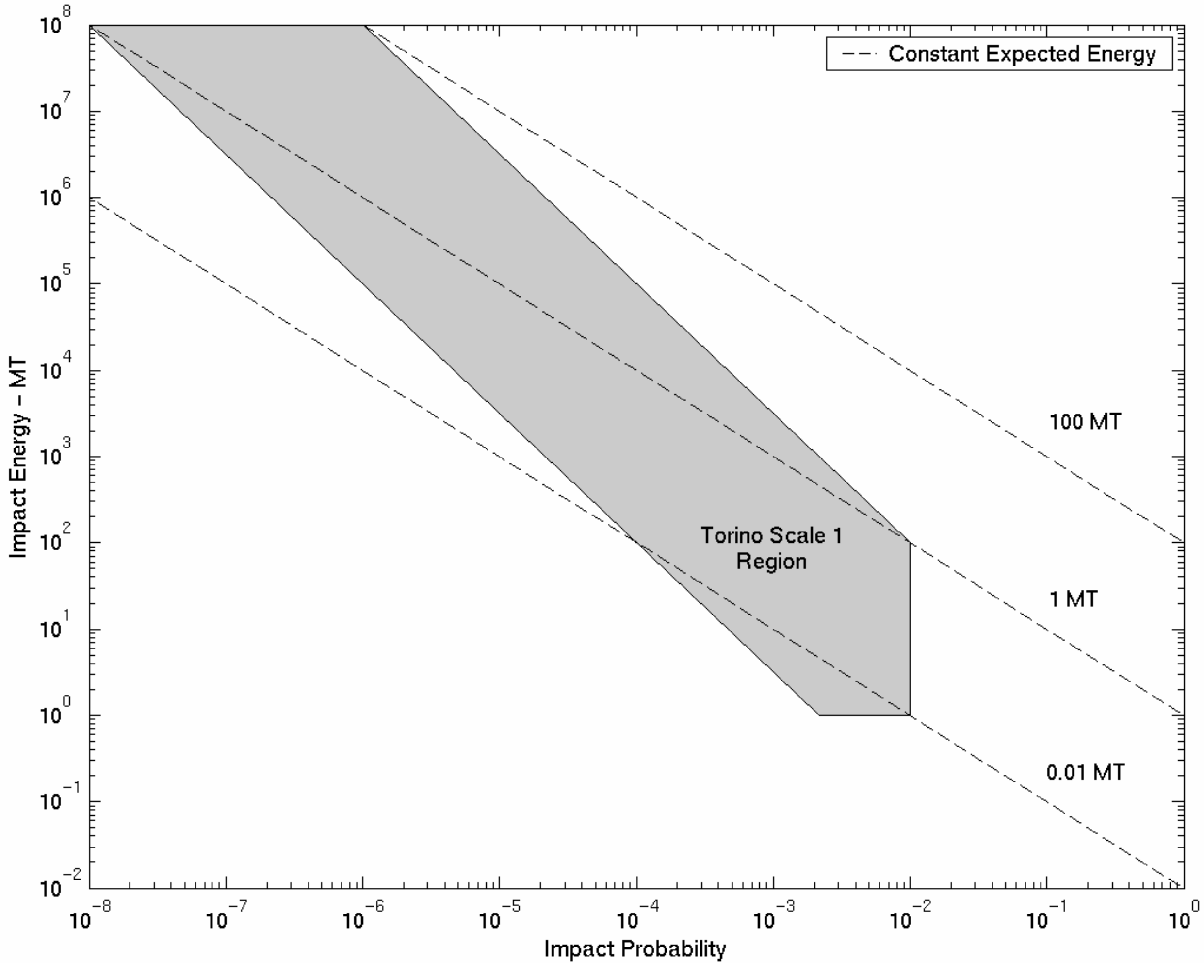

Fig. 1.— Lines of constant expected energy $\tilde{E}$ with values 0.01 MT, 1 MT, and 100 MT. The Torino Scale 1 region is shown for comparison.

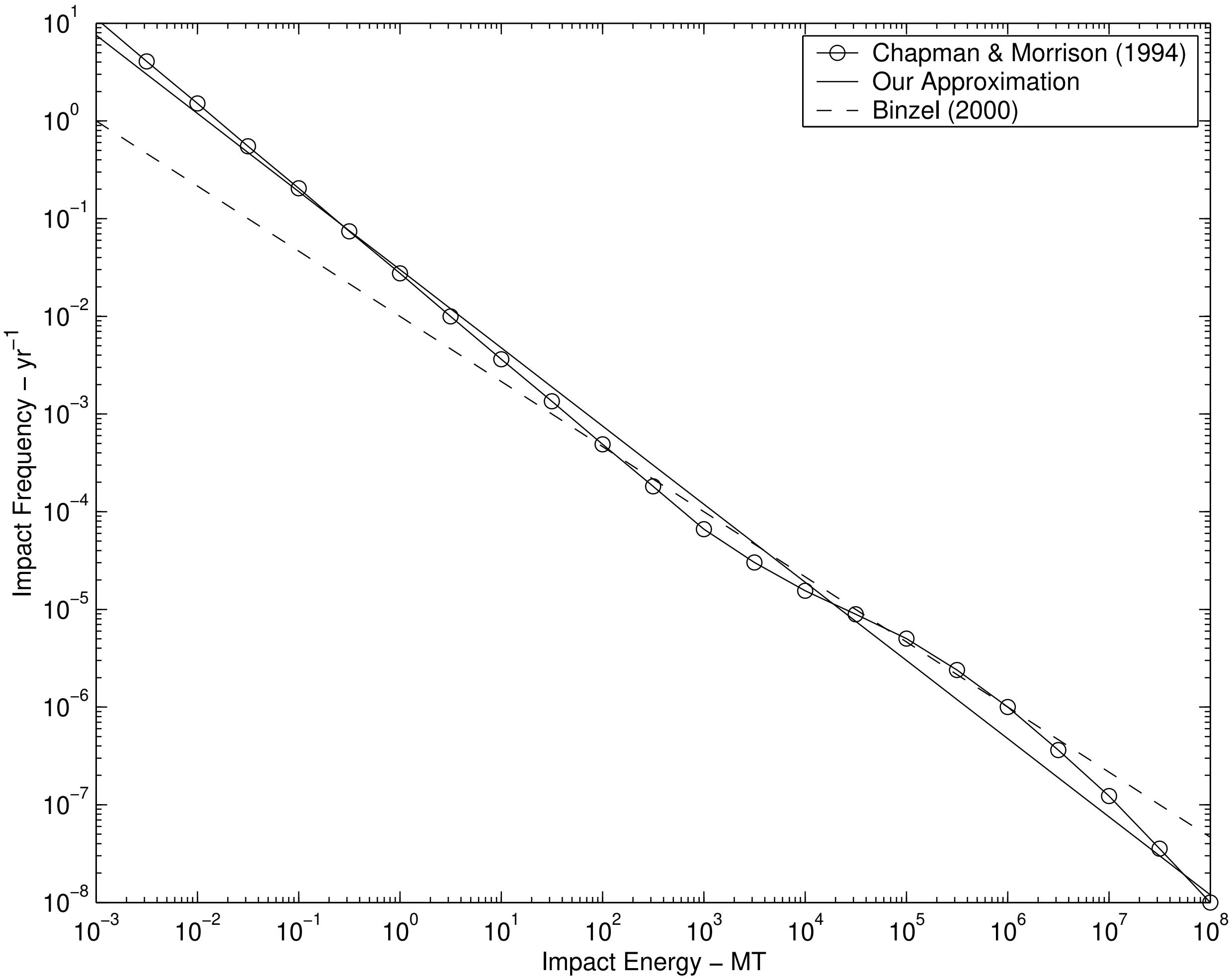

Fig. 2.— The frequency of Earth impact as a function of impact energy. The frequency includes all impacts with energies greater than the given energy.